

# Measurements of $F_2$ and $xF_3^\nu - xF_3^{\bar{\nu}}$ from CCFR $\nu_\mu$ -Fe and $\bar{\nu}_\mu$ -Fe data in a physics model independent way

U. K. Yang,<sup>7</sup> T. Adams,<sup>4</sup> A. Alton,<sup>4</sup> C. G. Arroyo,<sup>2</sup> S. Avvakumov,<sup>7</sup> L. de Barbaro,<sup>5</sup> P. de Barbaro,<sup>7</sup> A. O. Bazarko,<sup>2</sup> R. H. Bernstein,<sup>3</sup> A. Bodek,<sup>7</sup> T. Bolton,<sup>4</sup> J. Brau,<sup>6</sup> D. Buchholz,<sup>5</sup> H. Budd,<sup>7</sup> L. Bugel,<sup>3</sup> J. Conrad,<sup>2</sup> R. B. Drucker,<sup>6</sup> B. T. Fleming,<sup>2</sup> J. A. Formaggio,<sup>2</sup> R. Frey,<sup>6</sup> J. Goldman,<sup>4</sup> M. Goncharov,<sup>4</sup> D. A. Harris,<sup>7</sup> R. A. Johnson,<sup>1</sup> J. H. Kim,<sup>2</sup> B. J. King,<sup>2</sup> T. Kinnel,<sup>8</sup> S. Koutsoliotas,<sup>2</sup> M. J. Lamm,<sup>3</sup> W. Marsh,<sup>3</sup> D. Mason,<sup>6</sup> K. S. McFarland,<sup>7</sup> C. McNulty,<sup>2</sup> S. R. Mishra,<sup>2</sup> D. Naples,<sup>4</sup> P. Nienaber,<sup>3</sup> A. Romosan,<sup>2</sup> W. K. Sakumoto,<sup>7</sup> H. Schellman,<sup>5</sup> F. J. Sciulli,<sup>2</sup> W. G. Seligman,<sup>2</sup> M. H. Shaevitz,<sup>2</sup> W. H. Smith,<sup>8</sup> P. Spentzouris,<sup>2</sup> E. G. Stern,<sup>2</sup> N. Suwonjandee,<sup>1</sup> A. Vaitaitis,<sup>2</sup> M. Vakili,<sup>1</sup> J. Yu,<sup>3</sup> G. P. Zeller,<sup>5</sup> and E. D. Zimmerman<sup>2</sup>

(The CCFR/NuTeV Collaboration)

<sup>1</sup> University of Cincinnati, Cincinnati, OH 45221

<sup>2</sup> Columbia University, New York, NY 10027

<sup>3</sup> Fermi National Accelerator Laboratory, Batavia, IL 60510

<sup>4</sup> Kansas State University, Manhattan, KS 66506

<sup>5</sup> Northwestern University, Evanston, IL 60208

<sup>6</sup> University of Oregon, Eugene, OR 97403

<sup>7</sup> University of Rochester, Rochester, NY 14627

<sup>8</sup> University of Wisconsin, Madison, WI 53706

We report on the extraction of the structure functions  $F_2$  and  $\Delta xF_3 = xF_3^\nu - xF_3^{\bar{\nu}}$  from CCFR  $\nu_\mu$ -Fe and  $\bar{\nu}_\mu$ -Fe differential cross sections. The extraction is performed in a physics model independent (PMI) way. This first measurement of  $\Delta xF_3$ , which is useful in testing models of heavy charm production, is higher than current theoretical predictions. The ratio of the  $F_2$  (PMI) values measured in  $\nu_\mu$  and  $\mu$  scattering is in agreement (within 5%) with the predictions of Next-to-Leading-Order parton distribution functions (NLO PDFs) using massive charm production schemes, thus resolving the long-standing discrepancy between the two sets of data.

PACS numbers:12.38.Qk, 13.15.+g, 24.85.+p, 25.30.Pt UR-1586, submitted to *Phys. Rev. Lett.*

Deep inelastic lepton-nucleon scattering experiments have been used to determine the quark distributions in the nucleon. However, the quark distributions determined from muon [1] and neutrino [2] experiments were found to be different at small values of Bjorken  $x$ , because of a disagreement in the extracted structure functions. In this Letter, we report on a measurement of differential cross sections and structure functions from CCFR  $\nu_\mu$ -Fe and  $\bar{\nu}_\mu$ -Fe data. The neutrino-muon difference is resolved by extracting the  $\nu_\mu$  structure functions in a physics model independent (PMI) way. We also report on the first measurement of  $\Delta xF_3 = xF_3^\nu - xF_3^{\bar{\nu}}$ , which is used to test models of heavy charm production.

The sum of  $\nu_\mu$  and  $\bar{\nu}_\mu$  differential cross sections for charged current interactions on an isoscalar target is related to the structure functions as follows:

$$F(\epsilon) \equiv \left[ \frac{d^2\sigma^\nu}{dx dy} + \frac{d^2\sigma^{\bar{\nu}}}{dx dy} \right] \frac{(1-\epsilon)\pi}{y^2 G_F^2 M E_\nu} = 2xF_1[1 + \epsilon R] + \frac{y(1-y/2)}{1+(1-y)^2} \Delta xF_3. \quad (1)$$

Here  $G_F$  is the Fermi weak coupling constant,  $M$  is the nucleon mass,  $E_\nu$  is the incident neutrino energy, the scaling variable  $y = E_h/E_\nu$  is the fractional energy transferred to the hadronic vertex,  $E_h$  is the final state hadronic energy, and  $\epsilon \simeq 2(1-y)/(1+(1-y)^2)$  is the

polarization of the virtual  $W$  boson. The structure function  $2xF_1$  is expressed in terms of  $F_2$  by  $2xF_1(x, Q^2) = F_2(x, Q^2) \times \frac{1+4M^2x^2/Q^2}{1+R(x, Q^2)}$ , where  $Q^2$  is the square of the four-momentum transfer to the nucleon,  $x = Q^2/2ME_h$  (the Bjorken scaling variable) is the fractional momentum carried by the struck quark, and  $R = \frac{\sigma_L}{\sigma_T}$  is the ratio of the cross-sections of longitudinally- to transversely-polarized  $W$  bosons.

A similar equation for the case of muon scattering relates the cross sections to the structure functions. However, there are significant differences originating from the scattering on strange ( $s$ ) and charm ( $c$ ) quarks. The  $\Delta xF_3$  term, which in leading order  $\simeq 4x(s - c)$ , is not present in the  $\mu$  scattering case. In addition, in a charged current  $\nu_\mu$  interaction involving  $s$  (or  $\bar{c}$ ) quarks, there is a threshold suppression originating from the production of heavy  $c$  quarks in the final state. For  $\mu$  scattering, while there is no suppression for scattering from  $s$  quarks, there is larger suppression when scattering from  $c$  quarks since there are two heavy quarks ( $c$  and  $\bar{c}$ ) in the final state.

In previous analyses [2] of  $\nu_\mu$  data, light flavor universal physics model dependent (PMD) structure functions were extracted by applying a slow rescaling correction to correct for the charm mass suppression in the final state.

In addition, the  $\Delta xF_3$  term (used as input in the extraction) was calculated from a leading order charm production model. Recent calculations [3–5] indicate that there are large theoretical uncertainties in the charm production modeling for both  $\Delta xF_3$  and the slow rescaling corrections. Therefore, in the new analysis reported here, slow rescaling corrections are not applied, and  $\Delta xF_3$  and  $F_2$  are extracted from two-parameter fits to the data. We compare the values of  $\Delta xF_3$  to various charm production models. The extracted physics model independent (PMI) values for  $F_2^\nu$  are then compared with  $F_2^\mu$  within the framework of NLO models for charm production.

The CCFR experiment collected data using the Fermilab Tevatron Quad-Triplet wide-band  $\nu_\mu$  and  $\bar{\nu}_\mu$  beam. The CCFR detector [6] consists of a steel-scintillator target calorimeter instrumented with drift chambers, followed by a toroidally magnetized muon spectrometer. The hadron energy resolution is  $\Delta E_h/E_h = 0.85/\sqrt{E_h}$  (GeV), and the muon momentum resolution is  $\Delta p_\mu/p_\mu = 0.11$ . By measuring the hadronic energy ( $E_h$ ), muon momentum ( $p_\mu$ ), and muon angle ( $\theta_\mu$ ), we construct three independent kinematic variables  $x$ ,  $Q^2$ , and  $y$ . The relative flux at different energies, obtained from the events with low hadron energy ( $E_h < 20$  GeV), is normalized so that the neutrino total cross section equals the world average  $\sigma^{\nu N}/E = (0.677 \pm 0.014) \times 10^{-38}$  cm<sup>2</sup>/GeV and  $\sigma^{\bar{\nu} N}/\sigma^{\nu N} = 0.499 \pm 0.005$  [2]. After fiducial and kinematic cuts ( $p_\mu > 15$  GeV,  $\theta_\mu < 0.150$ ,  $E_h > 10$  GeV, and  $30 \text{ GeV} < E_\nu < 360 \text{ GeV}$ ), the data sample consists of 1,030,000  $\nu_\mu$  and 179,000  $\bar{\nu}_\mu$  events. Dimuon events are removed because of the ambiguous identification of the leading muon for high- $y$  events.

The raw differential cross sections per nucleon on iron are determined in bins of  $x$ ,  $y$ , and  $E_\nu$  ( $0.01 < x < 0.65$ ,  $0.05 < y < 0.95$ , and  $30 < E_\nu < 360$  GeV). Figure 1 shows typical differential cross sections at  $E_\nu = 150$  GeV (complete tables are available [7]). For all energies, the cross sections are in good agreement with NLO PDFs (with massive charm production schemes e.g., MRST99 [8] or CTEQ4HQ [9]). The dashed lines shows the predictions from the Thorne and Roberts Variable Flavor Scheme (TR-VFS) [4] QCD calculation using MRST99 extended [10] PDFs. This calculation includes an improved treatment of massive charm production. The QCD predictions, which are on free neutrons and protons, are corrected for nuclear [2], higher twist [11,12], and radiative effects [13]. Also shown are the predictions from a CCFR leading order (LO) QCD inspired fit used for calculation of acceptance and resolution smearing corrections. As expected from QCD, the CCFR cross section data exhibit a quadratic  $y$  dependence at small  $x$  for  $\nu_\mu$  and  $\bar{\nu}_\mu$ , and a flat  $y$  distribution at high  $x$  for  $\nu_\mu$ .

Next, the raw cross sections are corrected for electroweak radiative effects [13], the  $W$  boson propagator, and for the 5.67% non-isoscalar excess of neutrons over protons in iron (only important at high  $x$ ). Values of

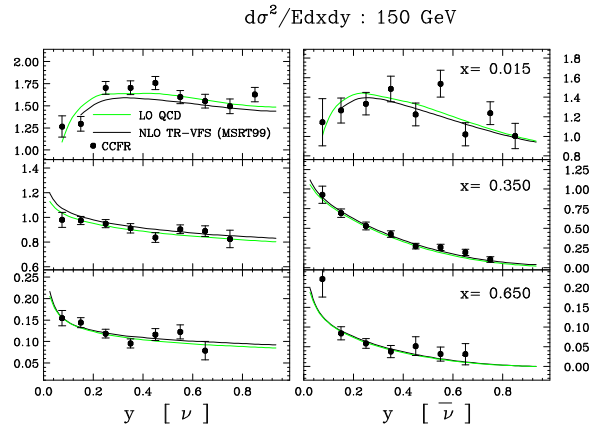


FIG. 1. Typical raw differential cross sections at  $E_\nu = 150$  GeV (both statistical and systematic errors are included). The CCFR data are in good agreement with the NLO TR-VFS QCD calculation using MRST99 PDFs (dashed line). The solid line is a CCFR LO QCD inspired fit.

$\Delta xF_3$  and  $F_2$  are extracted from the sums of the corrected  $\nu_\mu$ -Fe and  $\bar{\nu}_\mu$ -Fe differential cross sections according to Eq. (1). However, it is challenging to fit  $\Delta xF_3$ ,  $R$ , and  $2xF_1$  using the  $y$  distribution at a given  $x$  and  $Q^2$  because of the strong correlation between the  $\Delta xF_3$  and  $R$  terms, unless the full range of  $y$  is covered by the data. Covering this range (especially the high  $y$  region) is difficult because of the low acceptance. Therefore, we restrict the analysis to two-parameter fits.

Our strategy is to fit  $\Delta xF_3$  and  $F_2$  (or equivalently  $2xF_1$ ) for  $x < 0.1$  where the  $\Delta xF_3$  contribution is relatively large, while constraining  $R$  using the  $R_{world}^{\mu/e}$  [14] QCD-inspired empirical fit to all available electron and muon scattering data. The  $R_{world}^{\mu/e}$  fit is also in good agreement with NMC  $R^\mu$  data [1] at low  $x$ , and with the most recent theoretical prediction [12] for  $R$  (a NNLO QCD calculation including target mass effects). For  $x < 0.1$ ,  $R$  in neutrino scattering is expected to be somewhat larger than  $R$  for muon scattering because of the production of massive charm quarks in the final state. A correction for this difference is applied to  $R_{world}^{\mu/e}$  using a leading order slow rescaling model to obtain an effective  $R$  for neutrino scattering,  $R_{eff}^\nu$ . The difference between  $R_{world}^{\mu/e}$  and  $R_{eff}^\nu$  is used as a systematic error. Because of the positive correlation between  $R$  and  $\Delta xF_3$ , the extracted values of  $F_2$  are rather insensitive to the input  $R$ . In contrast, the extracted values of  $\Delta xF_3$  are sensitive to the assumed value of  $R$ , which is reflected in a larger systematic error. The values of  $\Delta xF_3$  are sensitive to the energy dependence of the neutrino flux ( $\sim y$  dependence), but are insensitive to the absolute normalization. The uncertainty on the flux shape is estimated by using the constraint that  $F_2$  and  $xF_3$  should be flat over  $y$  (or  $E_\nu$ ) for each  $x$  and  $Q^2$  bin.

Because of the limited statistics, we use large bins in

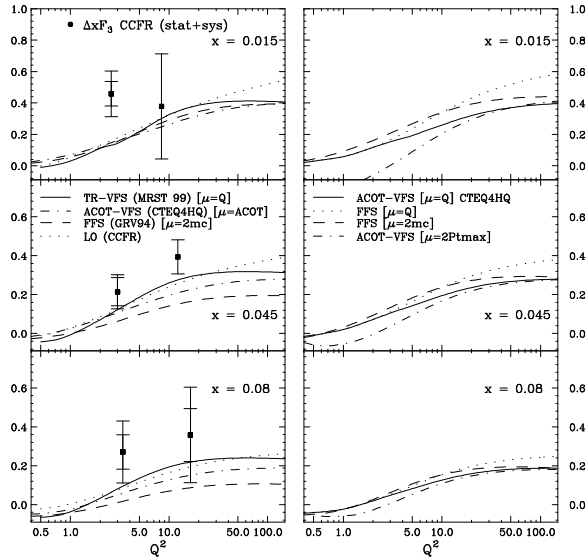


FIG. 2.  $\Delta xF_3$  data as a function of  $x$  compared with various schemes for massive charm production: (left) TR-VFS(MRST99), ACOT-VFS(CTEQ4HQ), FFS(GRV94), and the CCFR-LO (a leading order model with a slow rescaling correction); (right) Sensitivity of the theoretical calculations to the choice of scale.

$Q^2$  in the extraction of  $\Delta xF_3$  with bin centering corrections applied using the NLO TR-VFS calculation [4] with the MRST99 PDFs. Figure 2 (left) shows the extracted values of  $\Delta xF_3$  as a function of  $x$ , including both statistical and systematic errors, compared to various theoretical methods for modeling heavy charm production within a QCD framework. The three-flavor Fixed Flavor Scheme (FFS) [15] assumes that there is no intrinsic charm in the nucleon, and that all scattering from  $c$  quarks occurs via the gluon-fusion diagram. The concept behind the Variable Flavor Scheme (VFS) proposed by ACOT [5,16] is that at low scale,  $\mu$ , one uses the three-flavor FFS scheme, while above some scale, an intrinsic charm sea (which is evolved from zero) is introduced. The concept of the TR-VFS scheme [4] is similar, except that at intermediate scale it interpolates smoothly between the two regions. Both the FFS and VFS schemes have been implemented by KLS [3], ACOT, and Kretzer [17]. The last two implementations agree with each other, but not with KLS (there was a mistake in the KLS calculation) [18].

Shown are the predictions from the TR-VFS scheme (implemented with MRST99 PDFs and the suggested scale  $\mu = Q$ ) and along with the predictions from two other other NLO calculations, ACOT-VFS (implemented with CTEQ4HQ PDFs and their recent suggested scale  $\mu = m_c$  for  $Q < m_c$ , and  $\mu^2 = m_c^2 + 0.5Q^2(1 - m_c^2/Q^2)^n$  for  $Q < m_c$  with  $n = 2$  [5]), and the FFS (implemented with the GRV94 [19] PDFs and their recommended scale  $\mu = 2m_c$ ). Also shown are the predictions from the leading order QCD fit to the CCFR dimuon [20] data.

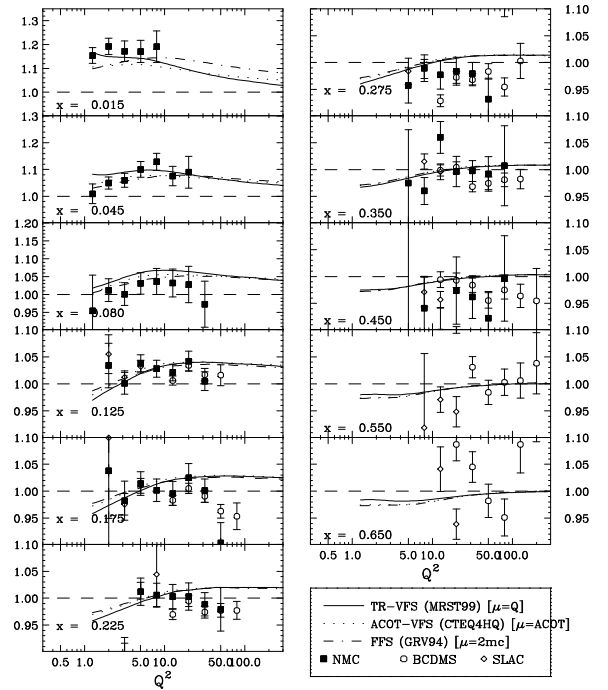


FIG. 3. The ratio of  $F_2^\nu$  (PMI) data divided by  $F_2^\mu$  (NMC or BCDMS) or  $F_2^e$  (SLAC). Both statistical and systematic errors are included. Also shown are the predictions of the TR-VFS (MRST99), ACOT-VFS (CTEQ4HQ) and FFS (GRV94) heavy flavor calculations.

Figure 2 (right) shows the sensitivity to the choice of scale. For example, the data do not favor the choice of scale,  $\mu = 2Pt_{max}$  in the ACOT-VFS calculation with CTEQ4HQ PDFs. This high scale (originally suggested by ACOT and used in the CCFR dimuon analysis [20]) implies that the calculation is in the four-flavor region even at  $x = 0.015$  and  $Q^2 = 1.0 \text{ GeV}^2$  (and yields large negative result). With reasonable choices of scale, all the theoretical models yield similar results. However, at low  $Q^2$ , our  $\Delta xF_3$  data is higher than all of the theoretical models. The difference between data and theory may be due to an underestimate of the strange sea at low  $Q^2$ , or from missing NNLO terms. The question of the strange sea would be addressed by a global NLO analysis which combines the neutrino data for dimuons,  $\Delta xF_3$  and  $F_2^\nu$ , with  $F_2^{\mu,e}$ .

As discussed above, values of  $F_2$  for  $x < 0.1$  are extracted from two-parameter fits to the  $y$  distributions. In the  $x > 0.1$  region, the contribution from  $\Delta xF_3$  is small and the extracted values of  $F_2$  are insensitive to  $\Delta xF_3$ . Therefore, we extract values of  $F_2$  with an input value of  $R$  and with  $\Delta xF_3$  constrained to the TR-VFS (MRST99) predictions. Fig. 3 shows the ratio of our  $F_2^\nu$  (PMI) measurements divided by  $(18/5)F_2^\mu$  (NMC [1] or BCDMS [21]) or  $(18/5)F_2^e$  (SLAC [22]) measurements [23]. The overall normalization errors of 2% (CCFR), and 2.5% (NMC) are not shown. Within 5%, the ratio is in agreement with the predictions of the

TR-VFS (MRST99), ACOT-VFS (CTEQ4HQ), and FFS (GRV94) calculations [24].

In the calculation of the theoretical predictions, we have also included corrections for nuclear effects [2]. As mentioned earlier, the extracted values of  $F_2$  from the two-parameter fits are insensitive to  $R$ . For example, if we perform simultaneous two-parameter fits to  $F_2$  and  $R$  (while keeping  $\Delta x F_3$  fixed to the TR-VFS (MRST99) values), the extracted  $R$  values at  $x = 0.01$  are smaller than  $R_{eff}^\nu$ , but  $F_2$  changes by only 2 ~ 3%.

In the previous analysis [2] of the CCFR data, the ratio of the extracted values of  $F_2^\nu$  (PMD) data divided by  $(18/5)F_2^\mu$  (NMC) at the lowest  $x = 0.015$  and  $Q^2$  bin were 20% higher than the predictions of the light-flavor PDFs such as MRSR2 [25] or CTEQ4M [9] (see Fig. 4). About 10% of the difference originates from having used a leading order model for  $\Delta x F_3$  versus using our new measurement. Another 6% originates from having used the leading order slow rescaling corrections, instead of using NLO massive charm production models. The remaining 3% originates from improved modeling of the low  $Q^2$  PDFs (which changes the radiative corrections and the overall absolute normalization to the total neutrino cross sections). For higher  $Q^2$  at  $x = 0.015$ , and for the next two  $x$  bins ( $x = 0.045$  and  $0.08$ ), the smaller difference between the PMI and PMD results is due to equal contributions from the  $\Delta x F_3$  and the difference in the slow rescaling corrections. For the higher  $x$  bins ( $x > 0.1$ ), the contribution of  $\Delta x F_3$  is small, and the slow rescaling corrections in the leading order model are the same as those with the NLO theories. Therefore, the NMC and CCFR data are in agreement at large  $x$  whether PMI or PMD structure functions are used in the comparison.

In conclusion, the ratio of  $F_2$  (PMI) values measured in neutrino-iron and muon-deuterium scattering are in agreement with the predictions of Next-to-Leading-Order PDFs (using massive charm production schemes), thus resolving the long-standing discrepancy between the two sets of data. The first measurement of  $\Delta x F_3$  is higher than current theoretical predictions.

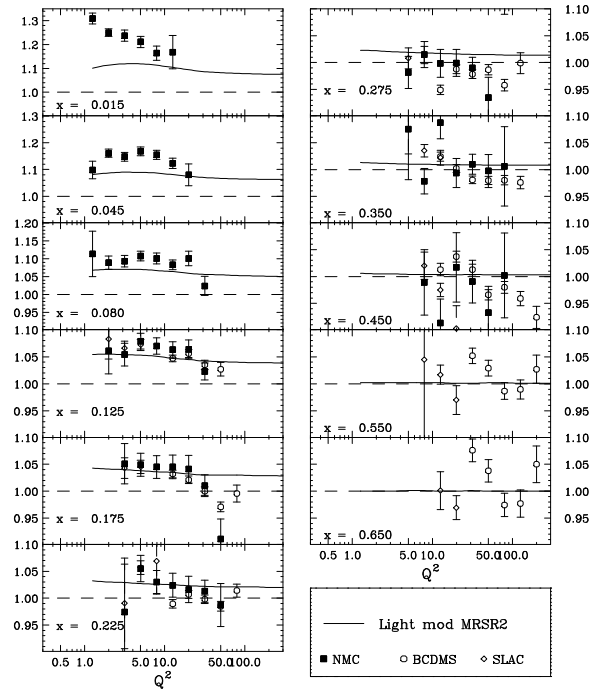


FIG. 4. The ratio of the previous  $F_2^\nu$  (PMD) data divided by  $(18/5)F_2^\mu$  (NMC or BCDMS) or  $(18/5)F_2^e$  (SLAC). Shown are the predictions of the MRSR2 light-flavor PDFs (the curves with CTEQ4M are very similar).

[1] M. Arneodo *et al.*, *Nucl. Phys.* **B483**, 3 (1997).  
[2] W. G. Seligman *et al.*, *Phys. Rev. Lett.* **79**, 1213 (1997).  
[3] G. Kramer, B. Lampe, and H. Spiesberger, *Z. Phys.* **C72**, 99 (1996).  
[4] R. S. Thorne and R. G. Roberts, *Phys. Lett.* **B421**, 303 (1998); RAL-TR-2000-048 (2000).  
[5] M. Aivazis, J. Collins, F. Olness, and W. K. Tung, *Phys. Rev.* **D50**, 3102 (1994).  
[6] W. K. Sakumoto *et al.*, *Nucl. Instr. Meth.* **A294**, 179 (1991); B. King *et al.*, *ibid* **A302**, 254 (1991).  
[7] <http://www-e815.fnal.gov/~ukyang/>; U. K. Yang, Ph.D. Thesis, University of Rochester (UR-1583, 2000).

[8] A. D. Martin *et al.*, *Eur. Phys. J.* **C14**, 133 (2000).  
[9] H. L. Lai *et al.*, *Z. Phys.* **C74**, 463 (1997).  
[10] For  $Q^2 < 1.2 \text{ GeV}^2$ , the MRST PDFs are extended according to the  $Q^2$  dependence of GRV94 PDFs.  
[11] U. K. Yang and A. Bodek, *Phys. Rev. Lett.* **82**, 2467 (1999).  
[12] U. K. Yang and A. Bodek, *Eur. Phys. J.* **C13**, 241 (2000).  
[13] D. Yu. Bardin and V. A. Dokuchaeva, JINR-E2-86-260 (1986).  
[14] L. W. Whitlow *et al.*, *Phys. Lett.* **B250**, 193 (1990).  
[15] E. Laenen *et al.*, *Nucl. Phys.* **B392**, 162 (1993).  
[16] M. Aivazis, F. Olness, and W. K. Tung, *Phys. Rev. Lett.* **65**, 2339 (1990).  
[17] S. Kretzer and I. Schienbein, *Phys. Rev.* **D58**, 094035 (1998).  
[18] F. Olness and S. Kretzer, Private communication.  
[19] M. Gluck *et al.*, *Z. Phys.* **C67**, 433 (1995).  
[20] A. Bazarko *et al.*, *Z. Phys.* **C65**, 189 (1995).  
[21] A. C. Benvenuti *et al.*, *Phys. Lett.* **B237**, 592 (1990).  
[22] L. W. Whitlow *et al.*, *Phys. Lett.* **B 282**, 475 (1992).  
[23] An empirical fit [1] to the SLAC, BCDMS, NMC  $F_2^d$  data is used for bin-center correction to these data.  
[24] Correction for the difference between  $\nu$ -Fe and  $\mu$ -Fe nuclear effects would make the agreement better (ref: C. Boros *et al.*, *Phys. Lett.* **B468**, 161, (1999)). Also, the predictions would increase by  $\approx 5\%$  at  $x = 0.015$ , if a strange sea which describes the  $\Delta x F_3$  data is used.  
[25] A. D. Martin *et al.*, *Phys. Lett.* **B 387**, 419 (1996).